Nanocomposites Made from Cellulose Nanocrystals and Tailored Segmented Polyurethanes

Maria L. Auad,[1] Mirna A. Mosiewicki,[1,2] Tara Richardson,[1] Mirta I. Aranguren,[2] Norma E. Marcovich[2]

[1]*Polymer and Fiber Engineering, Auburn University, Alabama*
[2]*INTEMA, Chemical Engineering Department, UNMdP-CONICET, Mar del Plata, Argentina*

Received 6 April 2009; accepted 27 July 2009
DOI 10.1002/app.31218
Published online 15 September 2009 in Wiley InterScience (www.interscience.wiley.com).

ABSTRACT: The effect of the addition of microcrystalline cellulose nanofibers into linear segmented polyurethanes (SPU) was investigated. The polymers were synthesized with 4,4-methylene-bisphenyldiisocyanate (MDI) and poly (tetramethyleneglycol) (PTMG) with 1,4-butanediol (BD) as chain extender. The nanocrystals were introduced during the PU polymerization, which resulted in cellulose nanofibrils covalently linked to the polymer. The interactions between the cellulose nanofibrils and the matrix lead to interesting changes in the behavior of the PU, with the hard segment (HS) phase being more affected by these interactions. SPUs with different contents of HS were synthesized to better understand these effects (23 to 45 wt %). Thermal, thermo-mechanical and mechanical characterization of the nanocomposites were performed. In general, the nanocellulose favored the phase separation between the soft and hard domains generating an upward shift in the melting temperatures of the crystalline phases, an increase in the Young's modulus and a decrease in deformation at break. Comparison of the unfilled polymer responses and that of the nanocomposites showed that by increasing cellulose content, increased dynamic storage and tensile modulus as well as melting temperatures and enthalpy of melting of the soft domains can be achieved. Addition of cellulose during the polymerization essentially erased the potential shape memory behavior originally displayed by some of the SPU. However, a sample prepared by adding the cellulose nanocrystals after the reaction showed that the mechanical properties were still improved, while the shape memory behavior of the polymer was preserved. J Appl Polym Sci 115: 1215–1225, 2010

Key words: block copolymers; nanocomposites; nanotechnology; polyurethanes; stimuli-sensitive polymers

INTRODUCTION

Shape memory polyurethanes are already well known for their distinct properties, such as easy processability, high resistance to organic solvents and solutions, long term stability against exposure to sunlight, consistent elastic properties and bio-compatibility. These materials have also the ability of "remembering" their original shape after being deformed and of recovering their original shape almost completely as a response to an external stimulus.[1]

The basis for the shape memory effect in segmented polyurethane (SPU) polymers is the presence of two separated molecular phases, formed by hard segments (HS) and soft segments (SS). Usually, there is a long range connectivity of the HS that leads to the percolation of the hard phase through the soft matrix.[2] The SS are polyols typically of molar mass 500–2000 or higher, whereas the HS are built from diisocyanates and chain extenders.[3] Depending on the types and compositions of the soft and HS and the preparation procedures, the structure-property relationships of polyurethanes are extremely diverse and can be tailored for using in different applications, from medical devices to intelligent fabrics or deployable components.[3–8]

However, the main disadvantage of using SPUs is their relatively weak recovery force.[10,11] Therefore, the SPUs are usually used in the cases where only free recovery or very low recovery force and mechanical strength are sought[9] thus, there are several applications for which the SPUs will not be viable. To increase the mechanical properties of these materials, SPU's have been reinforced with carbon or glass fibers, or ceramic filler particles.[10,12] Following this direction, the use of cellulose nanocrystals as reinforcement of SPU is a new approach, which is expected to enhance the elastic modulus using small nanoparticle loadings (up to 1 wt % in the present work), while still allowing reaching relatively large deformations. Recently, the use of cellulose crystals as nano-reinforcement was demonstrated.[13–16] The cellulose produces a remarkable

Correspondence to: M. L. Auad (auad@auburn.edu).
Contract grant sponsors: Polymer and Fiber Engineering Department, Department of Commerce (USA), Argentinean Science and Technology National Promotion Agency (ANPCyT), the National University of Mar del Plata (UNMdP), National Research Council of Republic Argentina (CONICET), John Guggenheim Foundation.

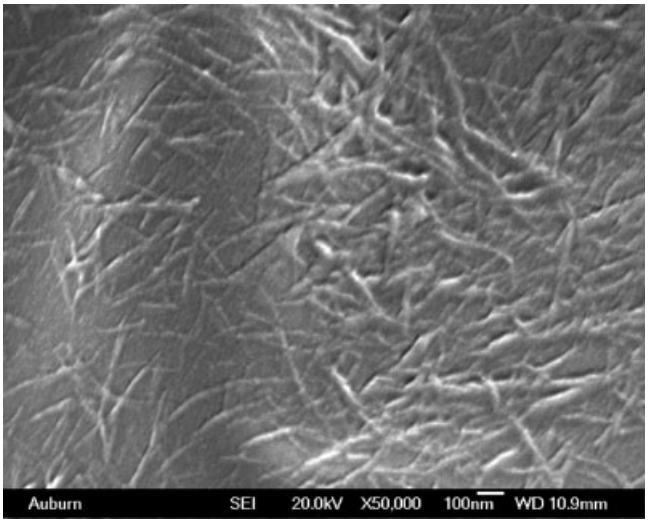

Figure 1 SEM image of the hydrolyzed cellulose fibers.

reinforcing effect, even at concentrations of a few percent. These natural fibers are an interesting alternative to mineral fillers in polymeric composites; their low cost, low density, high stiffness, and biodegradability constitute major incentives for the use of cellulose as reinforcement in the production of composites.

The purpose of this work is to investigate the properties and shape memory potential of composites prepared from cellulose nanocrystals and SPU's. The chemical structure of the linear polyurethanes was varied to obtain matrices with different SS molecular weights and hard to SS ratios. Both, the influence of the chemical structure of the matrix and the effect of the addition of the nanocellulose on the composites behavior were analyzed.

EXPERIMENTAL

Materials

Polyether glycol (PTMG) (TERATHANE®) with molar masses 650 and 2000 g/mol (PTMG 650 and PTMG 2000, respectively) were used. 4,4′-methylene-bis(phenyl isocyanate) (MDI) was purified by melting at 65°C and MDI dimers were removed using 25 mm diameter, 0.5 micron pore size syringe filters (from Millipore) before use. 1,4-butanediol (BD) and *N*,*N*-dimethylformamide (DMF), used as a solvent, were stored under 4 Å molecular sieves before use. All the reactives were purchased from Sigma-Aldrich.

Microcrystalline cellulose, MCC, (Avicel® PH-101MCC, FMC BioPolymer) was used to obtain cellulose nanocrystals.

Cellulose nanocrystals preparation

Aqueous suspensions of cellulose crystals were prepared from microcrystalline cellulose by acid hydrolysis.[16] The hydrolysis conditions were optimized by varying temperature and reaction time. The microcrystalline cellulose was mixed with sulfuric acid (50% w/v) in a ratio of microcrystalline cellulose to acid of 1 : 8.75 g/mL. The mixture was then held at 45°C for 2 h under strong stirring. The dispersion was completed by a further 10 min ultrasonic treatment (Ultrasonik 250, NEY). The suspension was diluted with an equal volume of water and washed repeatedly, each time the crystals were separated from the aqueous solvent by centrifugation (12,000 rpm, 10 min) until a pH 5 was reached. The final suspension was freeze-dried and redispersed in DMF using ultrasonic treatment.

The evaluation by X-ray diffraction of the samples shows that the crystallinity increased from 56–67% after hydrolysis. Optical microscopy of initial microcrystalline cellulose shows large agglomerates (around to 30 μm) formed by strong hydrogen bonding.[16] Scanning electron microscopy of the cellulose after acid treatment showed that the dimensions of the cellulose crystals are significantly smaller with diameters in the range of 50–100 nm and average aspect ratio above 50 (Fig. 1).

Synthesis of SPU's

Two series of SPU were synthesized by polymerization in DMF solution through a two step reaction. First, MDI and PTMG were dissolved in DMF. The mixture was allowed to react for 15 min at 80°C to prepare the polyurethane SS. These SS were subsequently chain extended with HS by the reaction of the BD in the second step. BD was added to the reaction mixture according to the desired MDI/BD ratio (see Table I) and reacted for 2–3 minutes until the solution became viscous. After this reaction step, the mixture was cast in open Teflon® molds and placed at 80°C for 24 h in a convection oven to evaporate the solvent. To obtain linear polyurethanes, in the synthesis of all the samples the isocyanate (NCO) to hydroxyl (OH) ratio was kept equal to 1.0. Additional information about the molar fractions and names allotted to the samples is included in Table I.

TABLE I
Composition of SPUs

	Sample designation	Hard segment content (wt %)	Relative mole composition		
			MDI	BD	PTMG
PTMG 650	SPU 650-48	48	2	1	1
PTMG 2000	SPU 2000-45	45	5	4	1
	SPU 2000-40	40	4	3	1
	SPU 2000-32	32	3	2	1
	SMPU 2000-23	23	2	1	1

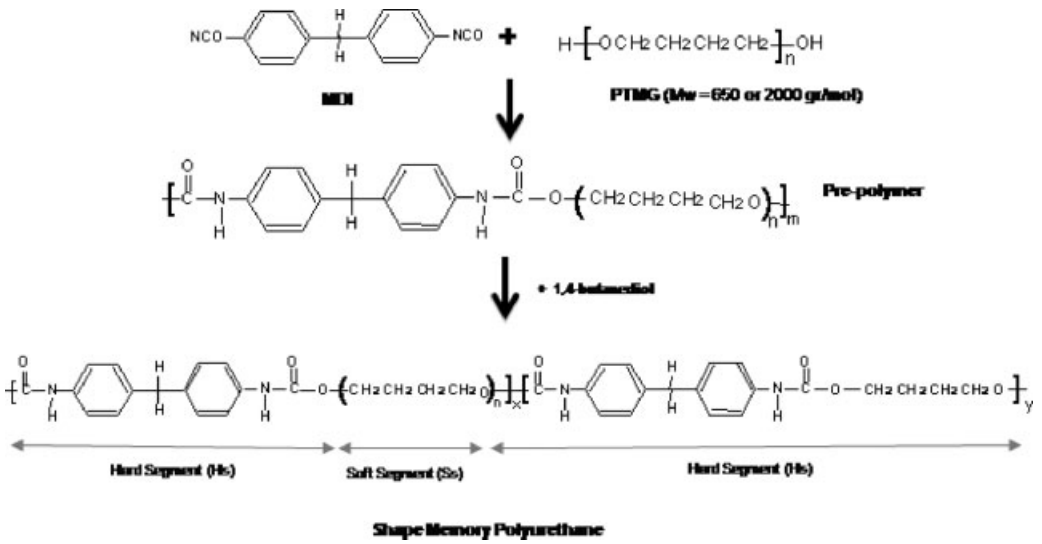

Figure 2 Scheme of the SPU synthesis.

A scheme of the structure of the samples and the different reaction steps is shown in Figure 2.

Preparation of reinforced SPU's

The cellulose composites were prepared in the same way as the unreinforced polyurethane, but adding a selected amount of hydrolyzed cellulose crystals in the first step of the reaction. The reinforcement was previously dispersed in DMF by ultrasonication and subsequently incorporated in the solution. Films containing 0.1, 0.5, and 1 wt % of cellulose crystals were obtained.

To separate the effect of the reaction between the cellulose crystals and the polyurethane from their reinforcing effect, another sample (SPU 2000-23) with 1 wt % cellulose was prepared by incorporating the crystals after the synthesis of the polyurethane. The neat thermoplastic SPU sample was dissolved in DMF and then, the nanofiller was added. The final film was obtained by casting the mixture in an open mold and drying it in a convection oven at 80°C for 24 h.

TECHNIQUES

Differential scanning calorimetry (DSC)

Thermal analyzes were carried out with a TA Instruments DSC 2920. The heating rate was 10°C/min and the enclosure was continuously purged with dry nitrogen.

Scanning electron microscopy (SEM)

A scanning electron microscope Philips model SEM 505 was used to observe the hydrolyzed cellulose fibers and the cryo-fractured surfaces of the SPU composites. Samples were previously coated with gold.

Dynamic mechanical analysis (DMA)

A dynamical mechanical analyzer (TA instruments, RSA III) was used to determine the thermo-mechanical response of specific samples. Tests were conducted using the temperature scan mode, tensile fixture, and a ratio of static to dynamic stresses of 1.2. The frequency of oscillation was fixed at 1 Hz. The specimens were cut to 20 × 5 × 0.5 mm and the linear dimensions were measured with an accuracy of ± 0.01 mm.

Tensile tests

Microtensile specimens of 5 mm × 25 mm were cut from the molded films and tested at room temperature using a universal testing machine (INSTRON 8501), in accordance with ASTM D 1708. Young's modulus (E) and yield stress (σ_y) were determined using a loading rate of 10 mm/min, while elongation at break (ε_b) was measured on tests performed at 100 mm/min. At least five replicates of each sample were measured, and the average values were reported.

Thermal cyclic tests were performed on microtensile specimens of 5 mm × 25 mm using a universal testing machine (INSTRON 8501) equipped with a heating chamber. Samples were first conditioned at 45°C for 10 minutes and subsequently elongated to 50% of the original length at a speed of 20 mm/min. Then the samples were cooled to −10°C and unloaded at a crosshead speed of 10 mm/min. Finally, the samples underwent the recovery process by heating for ten minutes at 45°C. The strain

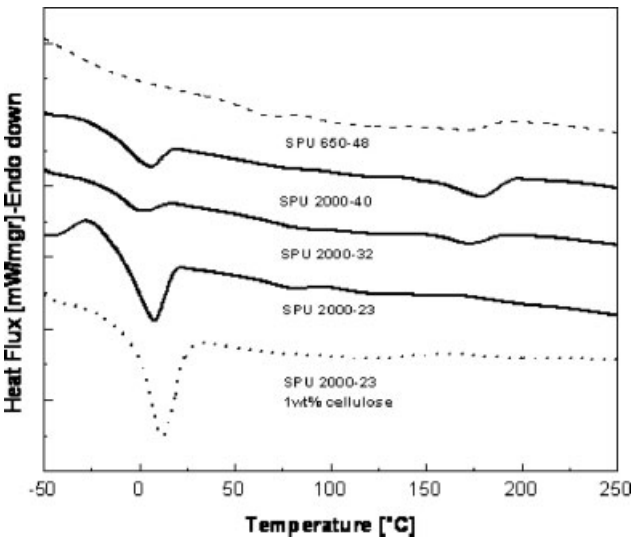

Figure 3 DSC curves of the SPUs containing different percentages of HS.

retained after unloading, and the residual strain of each cycle were used to calculate the fixity (R_f) and recovery (R_r) ratios from these tests, as indicated in the following equations:

$$R_f = \frac{\varepsilon_u}{\varepsilon_m} \times 100\% \quad (1)$$

$$R_r = \frac{\varepsilon_m - \varepsilon_p}{\varepsilon_m} \times 100\% \quad (2)$$

where ε_m is the maximum strain in the cycle (50%), ε_u is the residual strain after unloading at −10°C and ε_p is the residual strain after recovery.

To assess the dependence of the shape recovery with the number of cycles, this parameter was also evaluated as:

$$R_{r(N)} = \frac{\varepsilon_m - \varepsilon_p\ (N)}{\varepsilon_m - \varepsilon_p\ (N-1)} \times 100\% \quad (3)$$

where $\varepsilon_p(N)$ represents the residual strain after heating at 45°C in the Nth cycle.

RESULTS AND DISCUSSION

Characterization of unreinforced and reinforced segmented SPU

Thermal analysis (DSC)

To investigate the effects of polymer structure and interactions between the filler and the polymer on the nanocomposites behavior, thermal analysis was performed. Figure 3 shows the DSC scanning curves of neat SPU samples with different SS lengths and different HS content. A summary of the transition temperatures and enthalpy of melting is included in Table II.

In general, DSC curves of the neat SPU 2000-series show two clear melting peaks, one around ambient conditions (5–8°C) that corresponds to the melting of the semicrystalline SS and the other at higher

TABLE II
Thermal Properties of the Hard and Soft Segments in the SPU Reinforced with Different Percentages of Cellulose

	Soft segments			Hard segments	
Cellulose (wt %)	$T_{melting}$ (°C)	$\Delta H_{melting}$ (J/g)	$\Delta H_{melting}$ (J/g SS)	$T_{melting}$ (°C)	$\Delta H_{melting}$ (J/g)
		SPU 2000-45			
0	6.0	4.61	8.38	185.4	9.53
0.1	7.1	6.50	11.82		
0.5	9.6	15.16	27.56		
1	8.1	10.59	19.25		
		SPU 2000-40			
0	5.2	8.42	14.03	178.7	5.61
0.1	5.7	11.80	19.67		
0.5	8.2	13.99	23.32		
1	8.1	12.21	20.35		
		SPU 2000-32			
0	6.8	6.23	9.16	172.7	2.23
0.1	9.4	28.48	41.88		
0.5	11.6	26.51	38.99		
1	9.0	26.69	39.25		
		SPU 2000-23			
0	7.5	21.04	27.30	(a)	(a)
0.1	13.0	31.36	40.73		
0.5	11.3	31.35	40.71		
1	11.7	31.97	41.52		
[a]1	11.7	31.55	40.97		

[a] Cellulose incorporated after reaction, (a) It was not possible to measure these values.

temperatures (172–186°C), which corresponds to the HS domains. The existence of this window between the melting temperatures of the hard and soft domains is responsible for the shape memory characteristics of these materials. Wilkes and coworkers[17] studied this effect and concluded that at ambient conditions the hard blocks are incompatible with the soft blocks. This induces microphase separation of the HS by crystallization or liquid-liquid demixing.[17]

As expected, the morphology of SPU is strongly influenced by the molecular weight of the SS. Thus, in Figure 3 it can be seen that the SPU prepared with PTMG 650 (48 wt % of HS) shows no HS melting peak. However, the SPU with similar content of HS but prepared with PTMG 2000 (45 wt % of HS) presents clear melting transitions for both, the soft and HS. In the SPU prepared from PTMG 650, the SS chains are not long enough for contributing to incompatibility and phase separation, which facilitates the ordering inside the phases and leads to crystallization. This observation provides evidence that the degree of phase separation is increased by using SS of higher molecular weight.

On the other hand, the increase in HS content in the SPU prepared with PTMG 2000 produces a shift of the hard domains melting temperatures towards higher values and also an increase of the enthalpy of melting of the HS (Fig. 3 and Table II). The HS interaction among polymeric chains becomes stronger with the increase in the HS content in the SPU, resulting in higher HS-crystal melting temperatures and heats. The sample with 23 wt % of HS (SPU 2000-23) shows difficulty to pack the hard domains and consequently the thermal transition due to HS-melting is almost entirely erased from the DSC curve.

As it was expected, the increase in HS content (or decrease of the SS content) leads to smaller SS enthalpy of melting and a shift towards lower temperatures of the SS melting points (Fig. 3 and Table II). On one hand, the increase of HS would inhibit the mobility of the soft chains and interfere with the crystals formation and thus, less perfect crystals are formed (lower melting temperature). In agreement with this the heat of fusion of the SS crystals is also reduced with the increase of HS.

Thermograms of SPU 2000-40 containing different contents of cellulose added during the reaction are showed in Figure 4. The temperature position and heat flux involved in the transitions are also summarized in Table II. Reported results (Table II) show that a small addition of nanocrystals in the formulation produce large effects on the thermal behavior of the SPU 2000-series. For this part of the study, additional samples containing 0.1 wt % of nanocrystals were produced. The data shows that a small addition of cellulose shifts upwards the melting temperature of the SS and increases the heat of melting. This indicates that the cellulose favors the phase segregation of the polyurethane hard and soft phases. This effect reduces the interruption of SS crystallites by reducing order in the HS domains. Thus, the SS crystallites formed in the presence of the reinforcement are more perfect and melt at higher temperatures than in the unfilled samples. Note also that the SS-heat of melting for the two series with lower HS content seems to reach a maximum value at around 39-42 J/gSS, which would indicate that maximum segregation of the phases for this type of system has been achieved (at least in the conditions of this work). The segregation effect due to the cellulose addition is also present in SPU 2000-40 and SPU 2000-45, although in these cases the effect of the high concentration of HS interfering with the SS crystallization is more important.

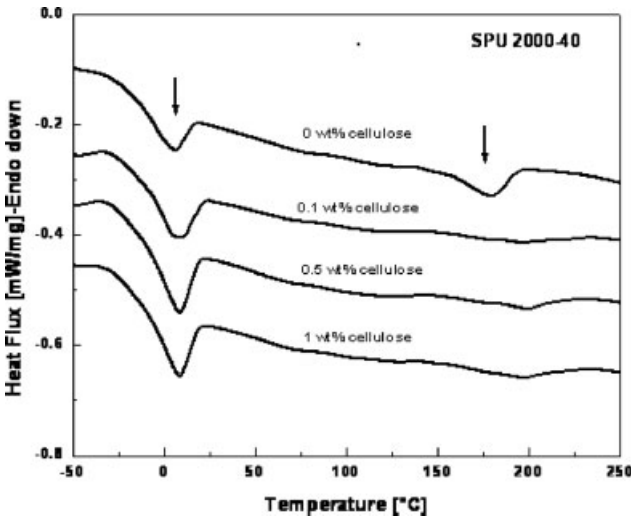

Figure 4 DSC curves of the SPU 2000-23 containing different concentrations of cellulose.

The melting endotherm corresponding to the HS phase in the neat polyurethanes is small, but noticeable in all the samples, except for the sample with the lowest HS content. The effect of adding cellulose nanocrystalites is the suppression of the endotherm. This suppression occurs because the polar nature of the cellulose crystals, which suggests a preferential association with the HS that are more polar than the PTMG SS. This association between the nanocellulose and the HS interferes with the hydrogen bonding that physically link HS together in crystalline domains, thus, prevent them from ordering. This effect has been reported previously in segmented PU reinforced with clay nanoplatelets.[18] In that case, the morphology study of the different neat PU and derived nanocomposites lead to the conclusion that the polar nanoparticles affected mostly the ordering of the HS phase, and that the crystallization of the

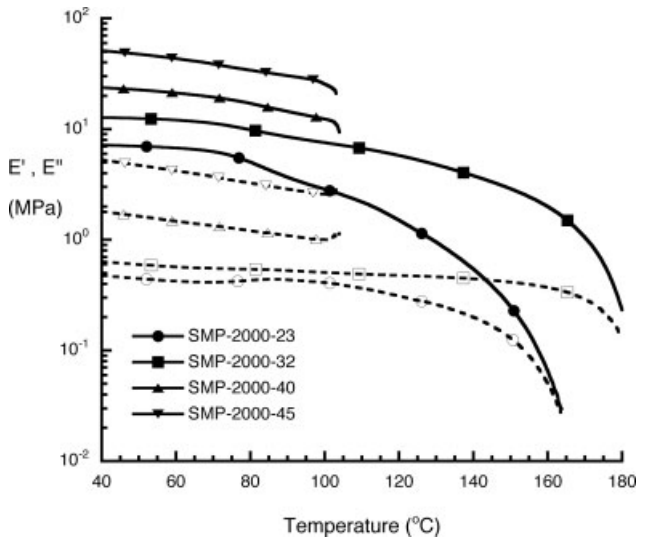

Figure 5 Storage and loss modulus as a function of the temperature for the SPUs with different percentages of HS. *E′*: filled symbols; *E″*: open symbols.

SS phase was favored through the increased phase segregation.

The DSC results for the reinforced SPU 2000-23 prepared with 1 wt % cellulose incorporated after the synthesis are also reported in Table II. The comparison of the results for this sample with those in which the cellulose was added during the reaction shows that the melting temperature and the heat (area of the peak) of the SS are not significantly affected by the preparation method. In both cases, there is a shift towards higher temperatures of the melting point of the SS with respect to the unreinforced polyurethane. The most reasonable explanation for this behavior is the presence of the filler that favors the phase separation as it was mentioned before. For both samples the amount of HS incorporated in the network is not enough for allowing detecting the high temperature melting.

Thermo-mechanical analysis (DMA)

Figure 5 shows the storage and loss moduli of the SPUs with different HS content. In the range of temperature analyzed the SPUs are above the glass transition and melting temperature of the SS. Regarding storage modulus, all the samples show a rubbery plateau, which extends up to 80–100°C. Above the HS melting temperatures, the SPU becomes soft producing a collapse of the network's structure. This is seen in the behavior of the samples containing 23 and 32 wt % of HS. If the content of HS is further increased, the cohesion of the material appears to be compromised and the samples collapse before the melting of the HS is completed. Additionally, and as it was expected, the higher content of HS leads to higher modulus in the material. The hard domains provide both physical crosslinking sites and filler like reinforcement to the SS matrix.[19] The corresponding loss modulus follows the same trend, but the decrease with temperature is less pronounced, at least for the samples with lower HS.

Figure 6 shows the storage and loss moduli as a function of the temperature of SPU 2000-23 with different cellulose contents (0, 0.5 and 1 wt %). The storage modulus curve corresponding to the pure matrix is typical for a thermoplastic material; below the melting temperature of the HS the storage modulus shows a relatively high value (a rubbery plateau is observed at low temperatures), which drops rapidly during the melting transition. Above the corresponding melting temperature, the material behavior is the expected for a thermoplastic in the terminal or flow zone. When the segmented PU is reinforced with a small percentage of fibrils, the polymer shows improved thermo-mechanical properties. The storage modulus increases largely with the cellulose addition. At 40°C the storage modulus is almost doubled by the addition of 1 wt % cellulose (7.5 and 13 MPa, respectively), while the flow region is shifted towards higher temperatures. There are two factors that can contribute to this behavior: (a) the incorporation of well dispersed nanofillers of high stiffness with high interfacial area and aspect ratio into a rubbery polymer produces considerable improvements in the modulus and (b) the incorporation of cellulose during the synthesis of the SPU can generate covalent bonds between the OH groups present in the cellulose and the isocyanate groups. This heterogeneous reaction has been already proved and discussed in a previous publication.[16] Even at a low percentage, these interfacial bonds can act as macro crosslinking-points that provide higher structural stability to the SPU at higher

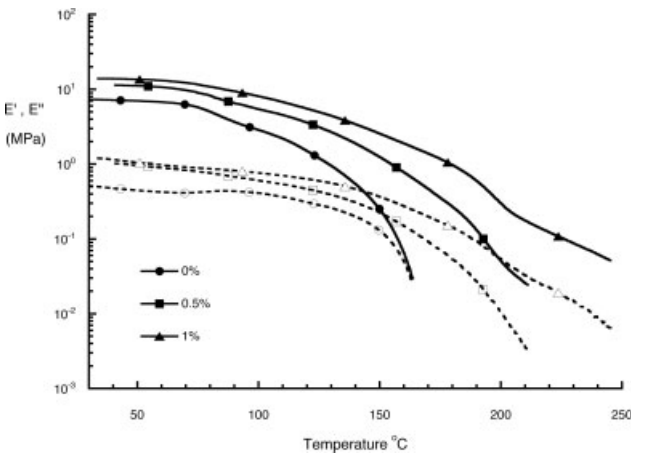

Figure 6 Storage and loss modulus as a function of the temperature for the SPU 2000-23 with different percentages of cellulose. *E′*: filled symbols; *E″*: open symbols.

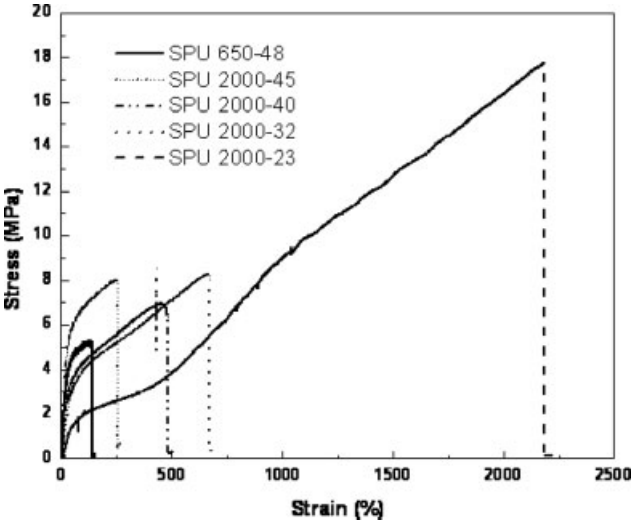

Figure 7 Tensile stress–strain curves for the SPUs with different contents of HS.

temperatures. Clearly, the elastic contribution increases at a higher rate than the loss modulus by the addition of the cellulose nanocrystals, thus the material become more rigid as reinforcement concentration increases.

TABLE III
Tensile Properties of the SPU Reinforced with Different Percentages of Cellulose

Cellulose (wt %)	Modulus (MPa)	Elongation at break (%)
	SPU 650-48	
0	31.84 ± 6.18	141 ± 17
0.5	31.11 ± 2.61	157 ± 25
1.0	31.47 ± 3.18	121 ± 6
	SPU 2000-45	
0	37.04 ± 1.13	203 ± 65
0.5	26.14 ± 2.42	16 ± 2
1.0	29.04 ± 4.93	37 ± 2
	SPU 2000-40	
0	15.71 ± 0.49	473
0.5	21.67 ± 2.36	79 ± 8
1.0	21.05 ± 5.30	114 ± 5
	SPU 2000-32	
0	9.60 ± 0.03	672
0.5	14.31 ± 0.48	115 ± 21
1.0	14.75 ± 0.78	68 ± 7
	SPU 2000-23	
0	4.54 ± 0.32	2165
0.5	6.47 ± 0.80	261 ± 43
1.0	6.56 ± 1.06	142 ± 28
[a]1.0	5.91 ± 0.50	971 ± 260

[a] Cellulose incorporated after reaction.

Mechanical analysis

The tensile properties of polyurethanes with different concentration of HS, length of SS and percentages of cellulose crystals were investigated by testing the composites at room temperature. The stress–strain curves show typical elastomeric behavior. Stress increases linearly with the strain at very small deformations (Fig. 7). As the stress is increased plastic deformation occurs. At this stage, the stress–strain curve deviates considerably from the Hookean behavior, since stress is redistributed by deformation (fragmentation) and reorganization of the HS. Finally, the polymer cannot bear the load anymore, and the material breaks. The steep upswing of the stress–strain curve (strain hardening) of SPU 2000-23 is caused by strain-induced crystallization of the PTMG SS. This is evidenced by the whitening of the material during testing. Although the other SPUs show some degree of strain hardening, no whitening is observed, because of the lower content of SS.

The values of the Young's modulus and elongation at break are reported in Table III. The Young's modulus of the polymers prepared with PTMG 2000 increase with increasing hard block content. As previously indicated, in these materials the HS domains act as reinforcement for the soft matrix formed by the SS.[2] Moreover, according to Wegner,[20,21] the logarithm of the modulus of a segmented copolymer follows a linear relationship with the volume fraction of HS. The present results plotted in the proposed form confirm this relationship (Fig. 8).

The strain at break of these polymers is very high for high SS content and decreases considerably as the HS concentration increases (SPU 2000-series). A larger elongation at break is often a sign of a greater extent of phase separation in segmented PUs.[22–24] Versteegen et al.[21] attributed this behavior to the easier deformation and reorganization of the thin crystalline

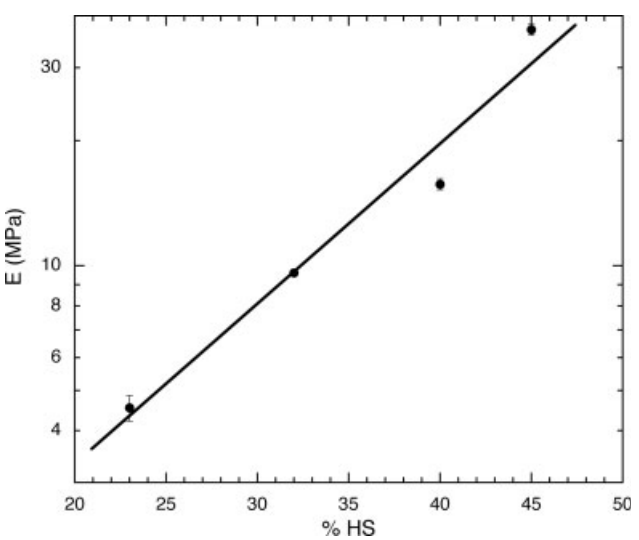

Figure 8 Young modulus versus hard segments percentage.

lamellae, so the stress is more evenly distributed over the SS. If a higher HS content is solubilized in the SS matrix, higher restrictions in the SS mobility are present in the material and consequently a marked decrease in ultimate elongation is observed.

The neat PU samples prepared with similar amounts of HS but different SS lengths (650-48 and 2000-45) show differences that can be tracked to the different length of the SS chains. The Young modulus (small deformations) of the two neat samples is little affected by the SS length. Small differences may be related to the different ability of the samples to phase separate and crystallize, despite the similar HS content. Regarding ultimate deformation, these properties are dominated by the length of the SS and thus, the values are higher for the SPU 2000.

As cellulose crystals are added in the first step of the PU synthesis, there exists the possibility of reaction between the SS chains and the cellulose through the action of the diisocyanate. Apparently, this does not hinder the SS chain capability for crystallization (DSC results), so one must infer that low range spatial mobility of the chains is not compromised by these bondings. Additionally, the presence of the cellulose nanocrystals with abundant hydroxyl groups affects the grouping and ordering of the HS, which is based in H-bonding attractions. Again, this observation is supported by the disappearance of the HS melting peak after cellulose addition. The composite mechanical properties respond to the balance of these two effects. The addition to the polymer of high modulus cellulose nanofibrils increases the modulus of the elastomers, but simultaneously, the cellulose crystals interfere with the formation of the HS, which leads to the reduction of the modulus. The analysis of the results of the tensile tests for the SPU 2000-series (except for the SPU 2000-45) indicate that the presence of a little amount of cellulose (0.5 wt %) produces a marked increase of the tensile modulus, although further addition of cellulose does not modify appreciably the previous result. The effect of adding rigid fibrils to the elastomer is the dominant effect. On the contrary, the SPU 2000-45 sample shows a reduction of the modulus when cellulose is added to the formulation. The interaction of the cellulose with the HS reduces the ordering of the HS and the addition of the rigid crystals does not compensate for this change.

The addition of cellulose crystals also affected notably the elongation at break of the samples. For the two samples with lower HS content (and lower modulus), the behavior is the expected for an elastomer reinforced with rigid particles, and thus, the higher the cellulose content, the lower the elongation at break. Just as with the variations in the modulus, the major change occurs by addition of a minimum amount of cellulose. For the SPU 2000 samples with higher HS content, the effect of addition of rigid particles is accompanied by the disruption of the HS domains. As in the other case the main effect is the reduction of elongation at break by incorporation of a minimum amount of cellulose. At 1 wt % of cellulose, the disruption of the HS domains can also favor the higher extensibility of the SS chains, leading to the increase of the deformation at break.

Further consideration of the SPU 2000-23 composite prepared by 1 wt % cellulose added after the polyurethane synthesis, allows addressing the effect of the cellulose addition without the complication of covalent interfacial bonding. Only physical interactions between the nanofibrils and the polymer are present in this sample, thus the modulus suffer an increase due to the addition of the rigid particles, while the elongation at break is reduced with respect to the unfilled polymer, but at a remarkably lower degree than in the case where chemical bonds to the cellulose crystals are involved (971% and 142% for the two composites, respectively).

In the case of the SPU 650-48, the addition of nanocelluose does not have such an important effect due to the unstructured (essentially not phase separated) morphology of the material.

Morphology

Scanning electron micrographs of the cryo-fractured films illustrate the morphology of the unfilled SPU films and its modification due to the presence of cellulose crystals (Fig. 9). The fractured surface of the neat matrix shows characteristic river marks and very little plastic deformation. In contrast, the sample with 1 wt % of cellulose shows a rougher fracture surface, suggesting the activation of new and different energy dissipating mechanisms. The advancing crack is deflected due to the presence of the rigid filler, generating a more tortuous cracking path. Another very interesting observation is that the image features are similar in all the area analyzed, indicating that the dispersion of the nanocellulose has been homogeneous at least at the level observed by SEM.

Shape memory effect

One of the most important features of shape memory materials is their ability to recover their original dimensions after being deformed and when a triggering signal is applied. In the shape memory testing of SPUs, deformation provides both the temporary shape and the driving force for shape recovery.[24] Besides, fixing is responsible for freezing the molecular segmental motion of the SS-rich phase to maintain the temporary shape, while recovery represents the reactivation of the mobility of the

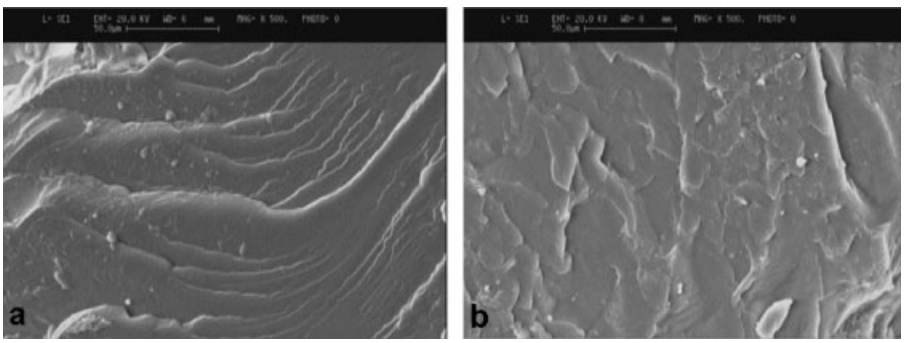

Figure 9 SEM images of the SPU 2000-23 containing: 0 wt % (a), and 1 wt % (b) of cellulose incorporated during the synthesis.

molecular segments necessary to return to the original shape.[25,26]

To study this behavior, cyclic thermal-mechanical tests were performed on these materials. Figure 10 shows tensile stress–strain curves with the thermal cycles for the SPU 2000-23 (which is representative of the behavior of all unreinforced synthesized PUs), while Figure 11 shows the corresponding curves for the same SPU containing 1 wt % of cellulose added after the reaction.

Rubber elasticity was observed within the temperature range between the melting temperature of the SS and the melting temperature of the HS because of the micro-Brownian motion of the SS and the restricted molecular motion due to the crystalline frozen phase. When stress is applied to the PU, the SS will be preferentially extended in the stress direction between fixed HS-domains.

When they were deformed in the temperature range between Tm_{SS} and Tm_{HS} and subsequently cooled below Tm_{SS} under a fixed maximum strain, the deformed shape was fixed because the micro-Brownian movement was frozen. However, in the present case, a small recovery occurred after unloading, the maximum deformation achieved (50%) could not be fully retained and fixity varied from 54–85% depending on the sample. When the samples were reheated to a temperature between Tm_{SS} and Tm_{HS}, the sample partially recovered the original length because of the elastic energy stored during the deformation (recovery was between 71 and 91% in the first cycle depending on the sample).

To have effective shape memory behavior, the HS domains must remain mostly unperturbed (inter- or intrapolymer chain attractions, such as hydrogen bonding or dipole–dipole interaction, must retain the physical crosslinking), but SS should be able to freely absorb external stress by unfolding and extending their molecular chains.[27–29] If the stress exceeds and breaks the interactions among HS, shape memory will be lost and original shape cannot be restored. Therefore, precise control of

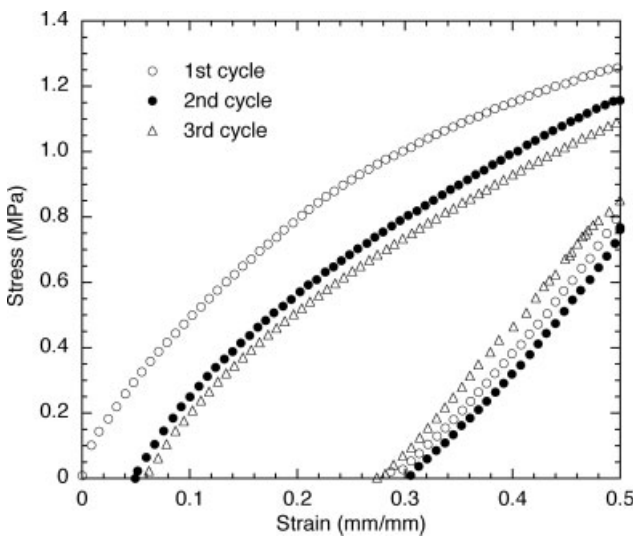

Figure 10 Tensile thermal cycles for the sample SPU 2000-23.

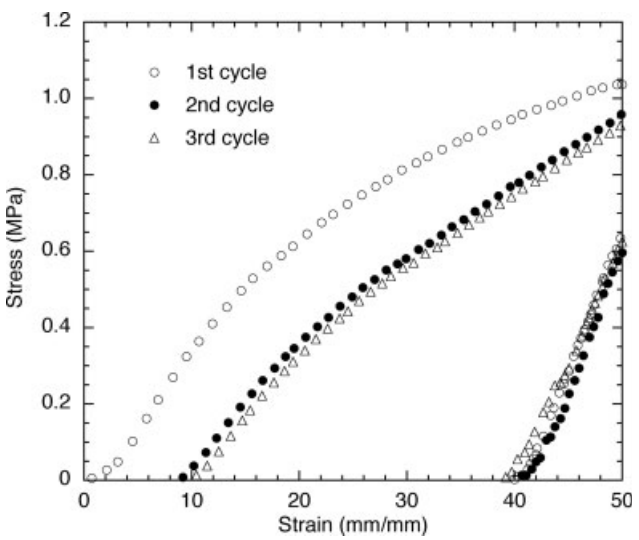

Figure 11 Tensile thermal cycles for the sample SPU 2000-23 with 1 wt % of cellulose added after the reaction.

TABLE IV
Shape Memory Properties of the SPU 2000-Series

HS (%)	Cellulose (wt %)	R_f	R_r	$R_r(N)$
	First cycle			
39	0	84.6	71.2	
32	0	62.9	80.6	
23	0	53.8	90.7	
23	1[a]	79.3	82.1	
	Second cycle			
39	0	67.9	71.2	100
32	0	61.8	79.9	99.3
23	0	55.8	88.3	97.1
23	1[a]	80.9	80.2	97.6
	Third cycle			
39	0	81.6	71.2	100
32	0	70.5	79.0	98.8
23	0	51.3	85.6	97.1
23	1[a]	78.2	80.0	99.8

[a] Cellulose incorporated after reaction.

composition and structure of hard and SS is very important to satisfy the conditions required for any application.[28]

In all cases, the stress–strain behavior of the first cycle was distinct from the behavior in subsequent cycles. This behavior is common in thermoplastic elastomers and is attributed to the effect of the thermo-mechanical history on chain conformation and phase domains distribution.[30,31] Thus, the shape recovery was also calculated with respect to the deformations of the previous cycle.

Table IV summarizes the shape memory properties for the SPU 2000 with different contents of HS and for the SPU 2000 reinforced with 1 wt % cellulose added after reaction. In general, the recovery and the fixity ratios did not vary significantly with increasing number of cycles. Figures 10 and 11 illustrate the response of the neat PU and the composite, clearly showing that after the first recovery the behavior is very repeatable. Therefore the shape recovery calculated with respect to the previous remnant deformation approaches unity. This implies that after the first deformation, which may produce some reordering in the phase distribution, the specimens behave almost as an ideal elastic network, the deformation of which is almost completely reversible.[1]

As expected, the fixity increased and recovery decreased (referred to the initial dimensions) with increasing of HS. The fixity ratio is directly proportional to the strain maintained after unloading (ε_u) that depends on the physical cross-links locking the programmed shape (HS). The strain recovered upon unloading the samples ($\varepsilon_m - \varepsilon_u$) depends on the modulus of the materials at the low temperature of the cycle (−10°C); the higher the modulus, the smaller the recovered strain, resulting in higher shape fixity.[24] The recovery ratio is inversely proportional to the residual strain after recovery (ε_p), which occurs at the high temperature of the cycle (45°C). At very high HS content there is a higher interaction among HS that form HS domains; the overall structure is more rigid and consequently less capable to recover its original shape. This behavior was also noticed by Lee et al.,[27] who linked it to microphase separation and density of physical cross-links affecting the dynamic properties of the PUs.

Finally, the neat SPU 2000-45 did not show shape memory behavior, because of the low volume of soft domains, which form the phase that can suffer relatively large deformation and recovery. This effect was previously observed by Lee et al.[27] for other SPU's prepared with more than 50 wt % of HS.

The comparison between the samples SPU 2000-23 without and with cellulose added after reaction (Table IV) indicates that the fixity increases significantly with the incorporation of cellulose while the recovery shows a smaller reduction. As mentioned above a higher modulus should lead to a higher fixity ratio.

On the other hand, the SPU 2000 composites prepared with cellulose crystals added during reaction did not show shape memory behavior. As it was previously indicated, cellulose can chemically react with MDI, and it strongly interferes in the formation of hard domains. The excess interactions between cellulose fibers and polyurethane chains results in structures unable to show shape memory behavior. At the high temperature part of the cycles (45°C), the low-ordered HS domains of the composites are easily perturbed by the tensile loads imposed and the material breaks at relatively low deformations.

Finally, the neat SPU 650-48 as well as the derived nanocomposites (0–1 wt % cellulose), could be deformed in a cyclic way only up to 20% maximum deformation. The fixity and recovery ratios were calculated (63 and 82% in the third cycle for the 1 wt % cellulose composite), but the sample is not promising as a shape memory material because of the small deformation capability of the base neat polymer.

As a final remark, it is clear that the obvious effect of the structure of the PUs (HS content and SS chain length) on the materials properties, the presence of cellulose and the testing temperature (as well as temperature history), all have an effect on the HS structure, phase segregation and ordering, which is determinant of the response of the materials.[32]

CONCLUSIONS

SPU's were synthesized as neat polymers and with the addition of small percentages of cellulose nanocrystals during the copolymerization reaction or incorporated after the polymerization. The incorporation of the cellulose induced changes in the

microstructure of the PU's, which affected the thermal and mechanical performance of the composite SPU. In general the nanocellulose favored the phase separation between the soft and hard domains generating an upward shift in the melting temperatures of the crystalline phases, an increase in the Young's modulus and a decrease in deformation at break.

The potential shape memory behavior of the SPU's was investigated for the neat and reinforced samples. As expected, the materials prepared with the long diol and having medium to low HS content were the polymers that showed shape memory effect.

The sequence of addition of the nanocellulose was paramount in the resulting properties. The incorporation of the nanocrystals after the polymer synthesis lead to less interaction of cellulose with the chemical structure of the polymer, but contributed to increase the modulus of the nanocomposite. The sample that incorporated the cellulose after the PU synthesis showed much higher deformability and retained the shape memory behavior of the base polymer. Addition of the cellulose nanocrystals during the synthesis increased modulus, reduced deformability and erased the shape memory behavior of the SPU's.

References

1. Li, F.; Zhang, X.; Hou, J.; Xu, M.; Luo, X.; Ma, D.; Kim, B. K. J Appl Polym Sci 1997, 64, 1511.
2. Sheth, J. P.; Klinedinst, D. B.; Pechar, T. W.; Wilkes, G. L.; Yilgor, E.; Yilgor, I. Macromolecules 2005, 38, 10074.
3. Ferrera, D. A. U.S. Pat. 6, 224, 610, 2001.
4. Benett, W. J.; Krulevitch, P. A.; Lee, A. P.; Northrup, M. A.; Folta, J. A. U.S. Pat. 5, 609, 608, 1997.
5. Lee, A. P.; Northrup, M. A.; Ahre, P. E.; Dupuy, P. C. U.S. Pat. 5, 658, 515, 1997.
6. Lee, A. P.; Fitch, J. P. U.S. Pat. 6, 086, 599, 2000.
7. Jeong, H. M.; Lee, S. Y.; Kim, B. K. J Mater Sci 2000, 35, 1579.
8. Yang, J. H.; Chun, B. C.; Cheng, Y.-C.; Cho, J. H. Polymer 2003, 44, 3251.
9. Wei, Z. G.; Sandström, R.; Miyazaki, S. J Mater Sci 1998, 33, 3743.
10. Liu, Y.; Gall, K.; Dunn, M. L.; Mccluskey, P. Smart Mater Struct 2003, 12, 947.
11. Lendlein, A.; Schmidt, A. M.; Langer, R. In Proceedings of the National Academy of Sciences of the Unites States of America; National Academy of Sciences, 2001; Vol. 98, 3, 842.
12. Gall, K.; Dunn, M. L.; Liu, Y.; Finch, D.; Lake, M.; Munshi, N. A. Acta Mater 2002, 50, 5115.
13. Wu, Q.; Henriksson, M.; Liu, X.; Berglund, L. A. Biomacromolecules 2007, 8, 3687.
14. Paillet, M.; Dufresne, A. Macromolecules 2001, 34, 6527.
15. Dufresne, A.; Vignon, M. R. Macromolecules 1998, 31, 2693.
16. Marcovich, N. E.; Auad, M. L.; Bellesi, N. E.; Nutt, S. R.; Aranguren, M. I. J Mater Res 2002, 21, 870.
17. Sheth, J. P.; Klinedinst, D. B.; Wilkes, G. L.; Yilgor, I.; Yilgor, E. Polymer 2005, 46, 7317.
18. Gregory, S. P. Ph.D. Dissertation, Massachusetts Institute of Technology, 2005.
19. Kim, H. D.; Huh, J. H.; Kim, E. Y.; Park, C. C. J Appl Polym Sci 1998, 69, 1349.
20. Wegner, G. I.; Legge, N. R.; Holden, G.; Schroeder, H. E., Eds. Thermoplastic Elastomers: A Comprehensive Review; Carl Hansser Verlag: New York, 1987.
21. Versteegen, R. M.; Kleppinger, R.; Sijbesma, R. P.; Meijer, E. W. Macromolecules 2006, 39, 772.
22. Abouzahr, S.; Wilkes, G. L. J Appl Polym Sci 1984, 29, 2695.
23. Wilkes, G. L.; Wildnauer, R. J Appl Polym Sci 1975, 46, 4148.
24. Kim, B. K.; Lee, S. Y.; Xu, M. Polymer 1996, 37, 5781.
25. Tobushi, H.; Hashimoto, T.; Ito, N. J Intell Mat Syst Struct 1998, 9, 127.
26. Kim, B. K.; Shin, Y. J.; Cho, S. M.; Jeong, H. M. J Polym Sci Part B: Polym Phys 2000, 38, 2652.
27. Lee, B. S.; Chun, B. C.; Chung, Y. C.; Sul, K. I.; Cho, J. W. Macromolecules 2001, 34, 6431.
28. Ratna, D.; Karger-Kocsis, J. J Mater Sci 2008, 43, 254.
29. Cho, J. W.; Jung, Y. C.; Chung, Y.; Chun, B. C. J Appl Polym Sci 2004, 93, 2410.
30. Boyce, M. C.; Socrate, S.; Kear, K.; Yeh, O.; Shaw, K. J Mech Phys Solids 2001, 49, 1323.
31. Koerner, H.; Price, G.; Pearce, N. A.; Alexander, M.; Vaia, R. A. Nat Mater 2004, 3, 115.
32. Lee, S. H.; Kim, J. W.; Kim, B. K. Smart Mater Struct 2004, 13, 1345.